Clays and Clay Minerals, Vol. 34, No. 6, 665–671, 1986.

CURVED SMECTITE IN SOILS FROM VOLCANIC ASH IN KENYA AND TANZANIA: A LOW-ANGLE X-RAY POWDER DIFFRACTION STUDY

S. J. VAN DER GAAST,[1] CHITOSHI MIZOTA,[2] AND J. H. F. JANSEN[1]

[1] Netherlands Intitute for Sea Research, P.O. Box 59
1790 AB Den Burg, Texel, The Netherlands

[2] Faculty of Agriculture, Kyushu University 46-02
Fukuoka 812, Japan

Abstract—Low-angle X-ray powder diffraction (XRD) measurements of soil samples, made at controlled relative humidities, showed the presence of major reflections at 20–33, 10–27, and 7–8 Å. The first reflection, which increased in intensity but did not shift in spacing with decreasing relative humidity, represents curved smectite layers. This spacing was also observed by high-resolution transmission electron microscopy. The value of 10–27 Å for the second reflection, the 001 reflection of smetite, is unusually high, probably due to poorly stacked, irregularly curved layers. The 7–8-Å reflection originates from kaolinite or dehydrated halloysite, which also contain curved layers. The more curved the layer structure of the smectite, the more difficult it is to detect this phase; therefore the XRD relative peak heights are not directly proportional to the percentages of the smectite.

Key Words—Curved layers, Kaolinite, Low-angle X-ray powder diffraction, Smectite, Soil clay, Relative humidity, Volcanic ash.

INTRODUCTION

Volcanic ash is generally thought to transform into other noncrystalline material by weathering in arid and semi-arid tropical regions. This transformation is seen by the absence of distinct 001 clay mineral reflections in X-ray powder diffraction (XRD) patterns of soils in East Africa (De Wit, 1978; Jager, 1982; Wielemaker and Wakatsuki, 1984; Mizota and van Reeuwijk, 1986). Many of these soils are thought to contain 2:1 phyllosilicates or incipient forms of phyllosilicates on the basis of their chemical composition, chemical-dissolution behavior, physical properties, and strong 02,11 XRD reflections (Mizota and van Reeuwijk, 1986). De Wit (1978) attributed a broad diffuse band between 10 and 14 Å to the presence of mixed-layer clay minerals. Allophane, a major weathering product of volcanic ash in humid regimes of cool temperate to tropical climatic zones, however, was not present (Wielemaker and Wakatsuki, 1984; Mizota and van Reeuwijk, 1986).

Low-angle XRD studies in this laboratory have yielded new data which have enabled us to determine the composition and structure of clay minerals in these soils and to augment our insight in weathering processes in volcanic ash soils in semi-arid and arid regions. From measurements on soil samples from Kenya and Tanzania we demonstrate here that the weak intensities of the 001 reflections of the phyllosilicates in the clay fraction of these soils originate from curved smectites.

SOIL SAMPLES AND METHODS

Soil samples

Samples of Kenyan and Tanzanian soils formed from peralkaline volcanic ash (Wielemaker and Wakatsuki, 1984; Mizota and van Reeuwijk, 1986) were studied. Brief descriptions of the sample localities, rainfall, sample-depth, soil horizon, and soil classification are listed in Table 1. For comparison, a halloysite of volcanic ash origin from Naike, New Zealand, and a smectite from a black soil in Addis Ababa, Ethiopia, were used as reference samples. The halloysite is pure, as shown by transmission electron microscopy (TEM), XRD, and acid-oxalate dissolution, a specific method for allophane extraction. The smectite contains traces of quartz, illite, and kaolinite.

Methods

Pretreatment. The soil samples were air-dried and passed through a 2-mm sieve. Air-dried material (10–20 g) was treated with 1 M NaOAc buffer solution (pH 5) to remove calcium carbonate and with H_2O_2 to remove organic matter. The residue was treated ultrasonically to break down aggregates. Small amounts of dilute NaOH solution were added to adjust the suspension to about pH 9. The clay fraction (<2 μm) was collected by repeated sedimentation and decantation and stored as a dilute NaCl suspension. In samples 4 and 5 this fraction contained substantial amounts of

Table 1. Description of soil samples.

Sample[1]	Locality and laboratory number	Approximate annual rainfall (mm)	Depth (cm)	Horizon	Classification	Reference
1	Mara, Kenya (1976/139)	1000–1600	7–23	A_2	Planosols	Mizota and Van Reeuwijk (1986)
2	South of Narok, Kenya (WW 145/5-2)	450–900	40–50	B_{2t}	Planosols	Mizota and Van Reeuwijk (1986)
3	Mukoma Hill, Serengeti, Tanzania (J-214)	400–500	120–150	B_{34ca}	Mollisols	Jager (1982)
4	Lemuta, Serengeti, Tanzania (SEK-NE-4)	<500	70–110	A_{14}	Mollisols	De Wit (1978)
5	Narok, Kenya (EAK 35-3)	800–1400	60–90	IIB_{22}	Andosols	Mizota and Van Reeuwijk (1986)
6	Kiambu, Kenya (EAK 2-1)	1200–1600	0–17	A_1	Andosols	Mizota and Van Reeuwijk (1986)

[1] Samples 1 and 2 are from soils with stagnant water; samples 3–6 are from well-drained soils.

primary minerals. To concentrate the clay minerals of these samples, the <0.2-μm fractions were collected using a centrifuge. Samples 4 and 5 were treated with DCB and subsequently with ⅓ M Na-citrate (pH = 7.3) at 100°C for 18 hr (Wada and Kakuto, 1983). Coatings of Fe and Al hydroxides commonly prevent parallel orientation of layer silicates. They are also incorporated in the interlayer space of swelling minerals (chloritization) in the soil during or after clay mineral formation, thus hampering the swelling of the layers used for identification in clay mineral analysis.

Transmission electron microscopy (TEM). A drop of well-suspended clay material was dried on a self-perforated microgrid. The grids were examined by high-resolution transmission electron microscopy (HRTEM) (JEM 100 B) at a direct magnification of 50,000×.

X-ray powder diffraction (XRD). For low-angle XRD, the method of Van der Gaast and Vaars (1981) was employed. The apparatus was modified with a computer-controlled divergence slit system, which provided a constant irradiated sample area independent of the angle of incidence and allowed measurements to be made as low as 0.5°2θ. CoKα radiation was produced by a long, fine-focus-type Co tube. Oriented specimens were obtained by suctioning Ca-exchanged clay suspensions onto polished, ceramic tiles. Instead of glycolation and K-saturation, the samples were equilibrated in a humidity generator at 100, 50, and 0% relative humidity (RH) which was maintained during the XRD measurements. This technique resulted in reproducible patterns of clay minerals and facilitated and improved the identification of swelling minerals. In 100% RH, smectites swelled to about 19.3 Å. In 0% RH, Ca-exchanged smectite lost most of its interlayer water and collapsed to about 11.6 Å. The XRD data were stored on a floppy disc and corrected for the Lorentz polarization factor and irradiated sample volume. To avoid errors in interpretation, the patterns of samples held at 100, 50, and 0% RH were plotted at comparable intensities, using the 001 kaolinite reflection as a reference. In the absence of a clear kaolinite reflection, some MoS_2 (reflection at 6.09 Å) was added as an internal standard.

Following routine analytical procedure currently used in soil clay mineralogy, XRD analysis was made of clay specimens saturated with Mg (50% RH), glycolated after Mg-saturation, saturated with K (50% RH), and saturated with K and heated to 300° and 550°C (0% RH). After Mg-saturation the characteristic XRD reflections of the swelling minerals and the low-angle reflections (see below) appeared at the same d-values at 100, 50, and 0% RH as those obtained after Ca-saturation. Heat treatments of the K-saturated samples, however, caused an increase of intensity and a peak shift of the low-angle reflections. Therefore, such

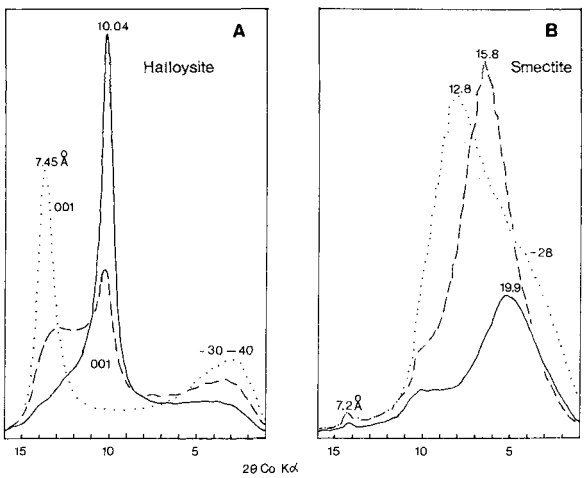

Figure 1. X-ray powder diffraction patterns of halloysite, Naike (A) and smectite, Ethiopia (B) in 100% relative humidity (RH) (solid line), 50% RH (dashed line), and 0% RH (dotted line). IS = internal standard (MoS_2).

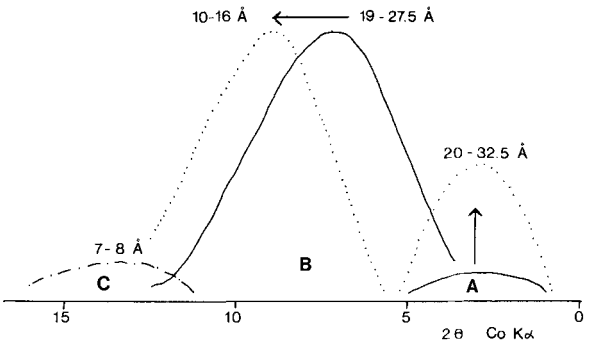

Figure 2. Schematic presentation of low-angle X-ray powder diffraction patterns. With decreasing relative humidity (RH), the low-angle reflection (A) increases in intensity and the smectite reflection (B) shifts to lower d-values; the kaolinite-halloysite reflection (C) is stable. For legends see Figure 1.

combination of heat treatments and glycolation did not provide a reliable means of identification of clay minerals in the soil samples discussed here. Consequently, the Ca-exchanged clay samples, measured at 100, 50, and 0% RH, as discussed in the present paper, were representative of all treatments.

RESULTS

X-ray powder diffraction

On the basis of XRD patterns made before and after DCB and ⅓ M Na-citrate treatment, no chloritization appeared to have taken place. The XRD pattern of all soil samples showed (1) a broad, low-angle reflection (27–33 Å) which increased in intensity with decreasing RH; (2) a broad reflection (19–27 Å) which shifted towards low d-values with decreasing RH, indicating the presence of a swelling clay mineral; (3) an illite reflection (10–10.6 Å); and (4) a kaolinite or halloysite reflection (7–8 Å) (Figures 3–5).

Reference clay minerals. Figure 1A shows the behavior of the low-angle reflection of the halloysite sample at 100, 50, and 0% RH. The 001 reflection of halloysite shifted from 10.04 to 7.45 Å with decreasing RH. The spacing of the broad reflection at 30–40 Å remained constant, but increased in intensity. The smectite sample behaved similarly. Its 001 reflection also shifted to lower d-values, and at 0% RH it overlapped a low-angle reflection (Figure 1B).

Soil samples. The XRD reflections of the soil samples at different RHs are shown schematically in Figure 2. The XRD reflection of the swelling clay mineral in sample 1 shifted from 24.5 to 13.1 Å with decreasing RH (Figure 3A; Table 2). At 50% RH a shoulder formed which at 0% RH developed into a well-defined, low-angle reflection at 33 Å. Sample 2 behaved similarly (Figure 3B); the spacings characteristic of a swelling mineral were somewhat larger and had no discrete maxima at 0% RH. Similarly, the XRD pattern of sample 3 (Figure 4A) at 0% RH showed only a broad hump between 10 and 20 Å. The principal reflection of the swelling mineral of sample 4 (Figure 4B) shifted from 19.5 Å at 100% RH to 16 Å at 50% RH. At 0% RH a partial collapse of the structure was indicated by the increased intensity between 10 and 16 Å; the main part of the reflection, however, remained at 16 Å. A low-angle reflection was expressed by an increase in intensity at about 27 Å. In sample 5 (Figure 5A), the most intense peak shifted from 19 Å at 100% RH to 16.5 Å at 50 and 0% RH. At 0% RH, the low-angle reflection was present as a shoulder at about 20 Å.

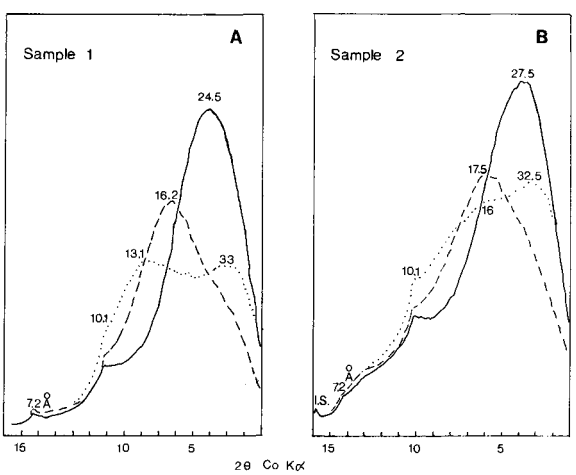

Figure 3. X-ray powder diffraction patterns of samples 1 (A) and 2 (B). For legends see Figure 1.

https://doi.org/10.1346/CCMN.1986.0340607 Published online by Cambridge University Press

Table 2. X-ray powder diffraction data for soil samples at different relative humidities (RH).

Sample	100% RH	50% RH		0% RH		
	Smectite + wave-structure	Smectite	Wave-structure	Smectite	Wave-structure	7–8-Å reflection
1	24.5	16.2	(sh)	13.1	33	–
2	27.5	17.5	(sh)	16	32.5	+
3	27	20	–	10–20 (b)	32.5	–
4	19.5	16	–	10–16 (b)	27	–
5	19	16.5	(sh)	10–16 (b)	20	+
6	27.5	–	24	–	26.5	+

sh = shoulder; b = broad; – = absent; + = present.

Sample 6 showed a weak reflection characteristic of a swelling clay mineral which shifted from 27.5 Å at 100% RH to 24 Å at 50% RH and to a shoulder at 21 Å at 0% RH (Figure 5B). At 0% RH, the low-angle reflection was a discrete peak at 26.5 Å.

The low-angle reflections of all clay samples were more intense that those of the two reference samples. The rates of increase of intensity with decreasing RH, however, were about the same. The d-values of the swelling clay mineral in the soil samples were generally too large for smectite. The kaolinite-halloysite reflection, present but weak in all samples, was broad in samples 2 and 5. In addition, weak illite reflections were present in the XRD patterns of all samples.

Transmission electron microscopy

Figure 6 (sample 3) shows particles having poor layer stacking, with d-values of about 15–20 Å, and irregular structures 20–40 Å in diameter that commonly display curved shapes. Clay particles showing these structures were noted in all samples. The structures were relatively unstable in the electron beam even at low voltages. Sample 3 was the only sample for which micrographs could be obtained without damage to the structure. Small amounts of micaceous minerals were also observed in all samples.

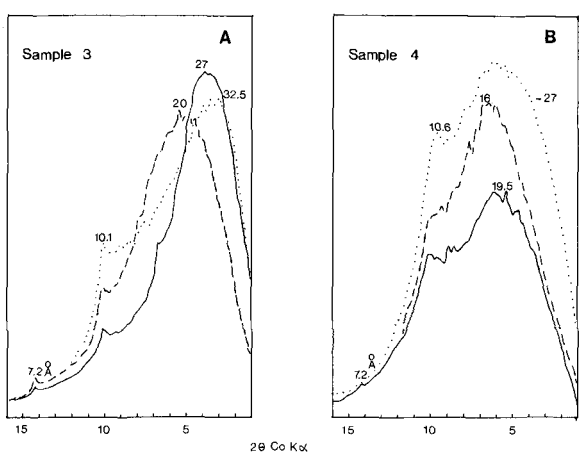

Figure 4. X-ray powder diffraction patterns of samples 3 (A) and 4 (B). For legends see Figure 1.

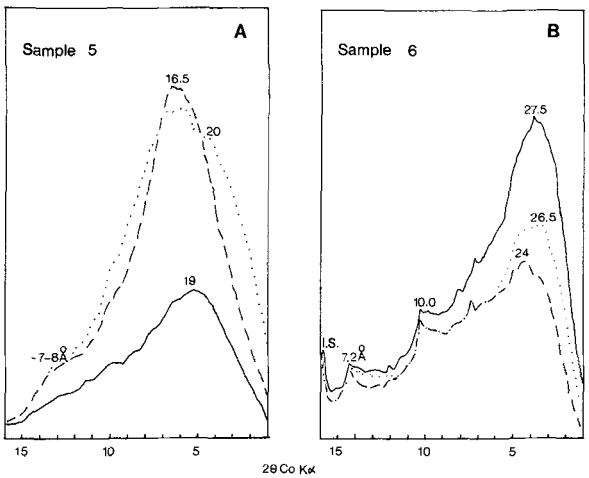

Figure 5. X-ray powder diffraction patterns of sample 5 (A) and 6 (B). For legends see Figure 1.

DISCUSSION

Reference samples

The low-angle reflection of the halloysite sample (30–40 Å) did not shift with decreasing RH (Figure 1A), indicating that it was not a 001 reflection. The intensity of the low-angle reflection, however, increased about twofold with decreasing RH. For the smectite reference sample, the rate of increase of the low-angle reflection was the same or somewhat higher (Figure 1). A comparable feature was observed in allophane, where a weak 34-Å reflection was noted at 100% RH, probably caused by allophane spherules of similar shape and size (van der Gaast *et al.*, 1985). At 0% RH this reflection increased eightfold in intensity due to increased ordering of the spherules caused by the removal of intercalated water molecules. Inasmuch as the reference samples contained no allophane, the low-angle reflection of the reference samples must have been due to the morphology of the phyllosilicate layers which resembled that of stacked allophane spherules.

Pauling (1930) predicted curved layers for kaolinite (1:1 layer) because the repeat distance of the octahedral sheet is larger than that of the tetrahedral sheet. For 2:1 layer clay minerals he predicted the same type of curving, because the constituent sheets are also not equivalent in size. Curved layers were also measured for antigorite (1:1 layer) by Zussman (1954) and Kunze (1956, 1958, 1961) who called this feature a superstructure. In these antigorites, spacings were noted at 16–19, 35–45, and 80–100 Å (Chapman and Zussman, 1959) and at 43.3 Å (Kunze, 1961). The latter value can be regarded as the distance between successive crests of a wave-shaped layer. We propose here that

https://doi.org/10.1346/CCMN.1986.0340607 Published online by Cambridge University Press

the low-angle reflections in the halloysite and smectite reference samples were caused by such wave-shaped layers. The increase in intensity with decreasing RH is attributed to a rearrangement of the layers by the removal of intercalated water molecules.

Soil samples

Low-angle reflection. The low-angle reflections in the XRD patterns of the soil samples cannot be attributed to admixed allophane because this mineral is not present (Mizota and van Reeuwijk, 1986). The soil samples are similar to the reference samples, in that their low-angle XRD peaks did not shift in d-value but increased in intensity with decreasing RH. Thus, these low-angle reflections, like those of the reference samples, represent curly phyllosilicate layers. Strong 02,11 and weak 001 reflections of oriented and non-oriented specimens indicate poor orientation of the phyllosilicate layers (Mizota and van Reeuwijk, 1986; Van der Gaast, unpublished results). The curvature of these layers was probably greater than those of the reference samples because the low-angle reflections were also more intense. The curvature is corroborated by the TEM observations of curved structures, 20–40 Å in diameter, in sample 3 (Figure 6), which agree fairly well with the d-value (32.5°) of the low-angle reflection recorded for this sample.

Because XRD reflections of illite and kaolinite-halloysite of the soil samples were present (see also Mizota and van Reeuwijk, 1986), the phyllosilicates characterized by curved layers must be the major component of the clay mineral fractions of the soil samples.

Swelling mineral reflection. The above results show that the layers did not collapse to spacings >10 Å, suggesting that the responsible swelling mineral was a 2:1 layer or a mixed-layer clay mineral. The irregular sequence of d-values, however, indicates that this mineral was not a mixed-layer phase. Thus, the swelling mineral must have been a smectite, however, its d-values must be higher than those usually reported. These high d-values reflect in part an apparent peak shift caused by an overlap of the low-angle reflection. Comparison of the d-values of the smectite reference sample (19.9, 15.8, and 12.8 Å at 100, 50, and 0% RH, respectively) with the d-values measured for Ca-exchanged Wyoming montmorillonite, which shows no measurable low-angle reflection (19.3, 15.4, and 11.6 Å; Van der Gaast and Kühnel, 1986) indicates apparent peak shifts of 0.6, 0.4, and 1.2 Å at 100, 50, and 0% RH, respectively. Correcting the d-values of soil samples 1–3 and 6 for these apparent shifts, however, gives spacings which are still much too large for smectite. This is also true if we consider that the overlap of the low-angle reflection is somewhat stronger than that of the smectite sample. For samples 4 and 5, the corrected d-values recorded at 100 and 50% RH, but not at 0%

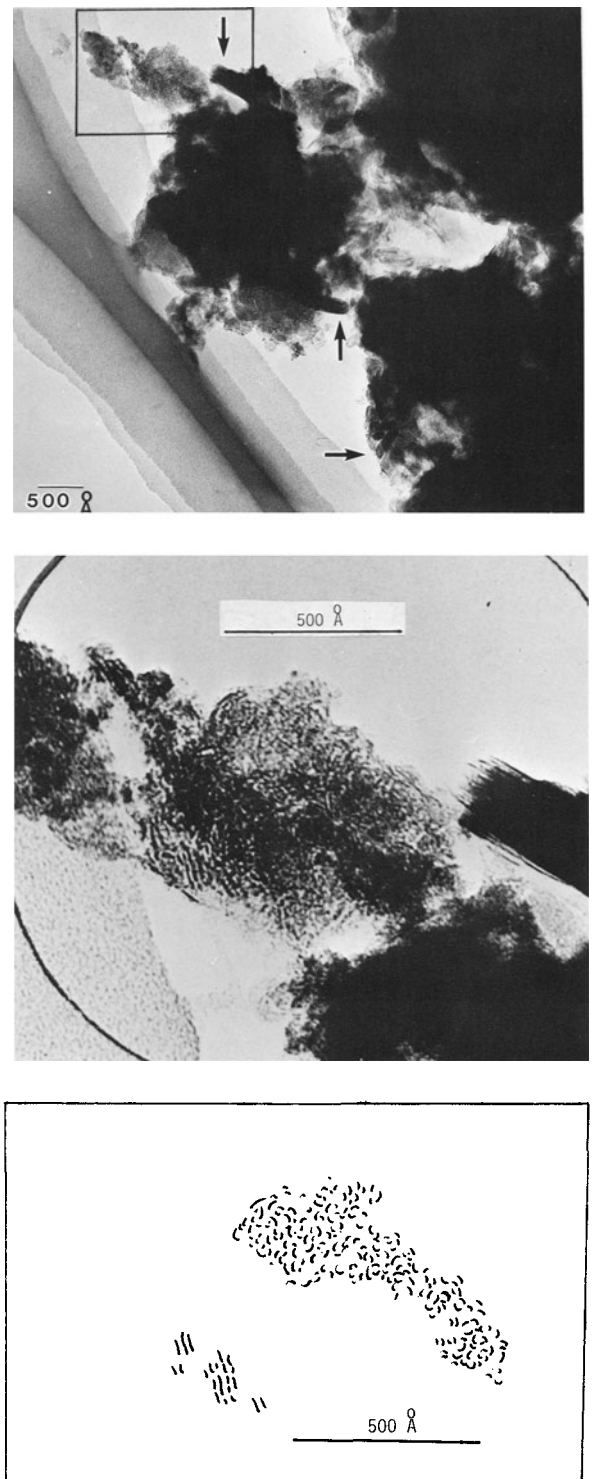

Figure 6. Transmission electron micrograph of sample 3. Arrows indicate areas having curved structures. (Middle) enlarged area from upper figure (rectangle) showing extended layers and curved structures. (Lower) drawing of the transparent parts of the same particles showing spacings of 20–40 Å at the top and 15–20 Å at the bottom.

https://doi.org/10.1346/CCMN.1986.0340607 Published online by Cambridge University Press

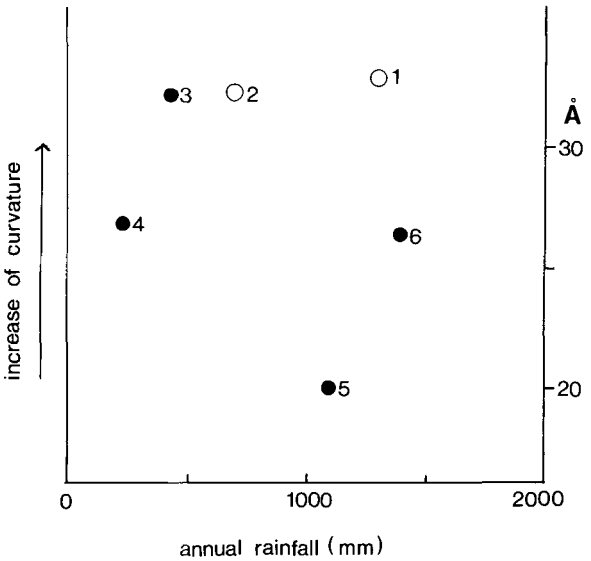

Figure 7. Relation of the low-angle reflection, representing curvature of smectite layers to annual rainfall. The spacing of the curvature is independent of annual rainfall. ○ = soils with stagnant water regime, ● = well-drained soils. Numbers in the figure correspond to those in Table 1.

RH, approximate the values of smectite. For all samples having corrected spacings still too large for smectites, a hump is present at 10–16 Å, pointing to an incomplete collapse of layers. This interpretation is corroborated by layer spacings of 15–20 Å in the TEM image of sample 3 (Figure 6). Ca-exchanged smectite should show a spacing of 10–11 Å due to dehydration caused by the vacuum in the specimen chamber of the electron microscope.

Because the observed d-values are too large for smectite (because of the incomplete collapse of the layers at 0% RH in all samples) and because of the irregularity and strong curvature of the layers, the swelling mineral in the soil samples must have been a smectite having expanded spacings at most humidities. These large spacings are probably due to poor stacking of the phyllosilicate layers of the smectite, irregularly curved in sequential layers. Possibly, the curvature originates from a replacement of Si in the tetrahedral sheet, a feature which is known for serpentine, a curved 1:1 layer mineral (Roy and Roy, 1954; Gillery and Hill, 1959).

Although smectite was present in large amounts, curvature of layers led to poor orientation and weak 001 reflections in XRD patterns. Consequently, the curved smectite is poorly ordered along the *c*-axis due to a poor stacking of layers. The strong 02,11 reflection, however, indicates that the smectite is well ordered along the *a* and *b* axes; the atomic arrangement within the separate layers is very regular. The smectite cannot therefore be regarded as an incipient mineral.

Kaolinite-halloysite. The broad XRD reflection at 7–8 Å in samples 2, 5, and 6 possibly represents kaolinite or dehydrated halloysite having slightly expanded layers. Expanded layers have also been found in a halloysite from New Zealand. TEM observations of this halloysite show curved layers having spacings of 8.1 Å, which is consistent with XRD measurements of broad reflections between 7.44 and 8.12 Å (McKee *et al.*, 1973). Therefore, the large spacings of kaolinite-halloysite in the clay samples 2, 5, and, possibly 6 are also likely due to curvature.

Occurrence of curved smectite

Figure 7 shows that the degree of the curvature of the smectite layers is independent of the annual rainfall of the sample sites. The chemical composition of the porewater of the soils is possibly an important factor in the formation of curved-layer minerals. The relatively weak 001 smectite peaks in samples 4–6 suggest the presence of relatively small amounts of smectite; however, because curvature also leads to weak 001 reflections and these three samples contain the most highly curved smectites, smectite may be most abundant in these samples. The only quantitative inference is that sample 3 contains the smallest amount of smectite. Its curvature resembles that of samples 1 and 2, but its low-angle XRD peak is weaker; compared to samples 4–6, its low-angle peak intensity is similar but the layer curvature is less (Figure 7). Therefore, the more curved the smectite, the more difficult it is to detect; the relative peak height does not appear to be proportional to the percentages of smectite.

SUMMARY AND CONCLUSIONS

The low-angle XRD technique reported here, coupled with the divergence slit technique and RH control used in these studies, has allowed new properties of soils to be examined which have previously been overlooked. Smectite is the major weathering product in samples from volcanic ash soils in the Great Rift Valley, East Africa. The 2:1 layers of this mineral are curved causing (1) weak 001 smectite reflections and (2) expanded layer spacings generally producing d-values that are too high for this reflection. For this curved mineral the intensity of the 001 reflection is not proportional to its content in a sample.

The curved smectite formed in arid and semi-arid tropical areas, in both soils in stagnant water-regimes and in well-drained soils. These occurrences are in contrast with the current view that such environments produce mainly noncrystalline weathering products. Because all of the examined samples appear to contain a considerable amount of smectite, this clay mineral is probably far more abundant in volcanic ash soils than has been generally believed. There is no reason to believe that the presence of curved minerals is restricted to this type of soils, and the low-angle XRD

technique may be of great importance in studying the physical and chemical behavior of soils and sediments.

ACKNOWLEDGMENTS

The authors thank K. Wada for stimulating discussions and for revising the manuscript, S.-I. Wada for technical assistance in electron microscopy, and C. M. Oomens-Meeuwsen and A. J. Vaars for technical assistance in X-ray powder diffraction. Soil samples were provided by the International Soil Reference and Information Centre, Wageningen, The Netherlands, and by W. G. Wielemaker, Department of Soil Science and Geology, Agricultural University, Wageningen, The Netherlands.

REFERENCES

Chapman, J. A. and Zussman, J. (1959) Further electron optical observations on crystals of antigorite: *Acta Crystallogr.* **12,** 550–552.

De Wit, H. A. (1978) Soils and grassland types of the Serengeti plain (Tanzania): Their distribution and interrelations: Ph.D. Thesis, Agricultural University, Wageningen, The Netherlands, 300 pp.

Gilley, F. H. and Hill, V. G. (1959) X-ray study of synthetic Mg-Al serpentines and chlorites: *Amer. Mineral.* **44,** 143–152.

Jager, Tj. (1982) Soils of the Serengeti woodlands, Tanzania: *Agric. Res. Rep.* 912, PUDOC, Wageningen, 239 pp.

Kunze, G. (1956) Die gewelte Struktur des Antigorites. I: *Z. Kristallogr. Kristallgeom.* **108,** 83–107.

Kunze, G. (1958) Die gewelte Struktur des Antigorites. II: *Z. Kristallogr. Kristallgeom.* **110,** 282–320.

Kunze, G. (1961) Antigorit. Strukturtheoretische Grundlagen und ihre Bedeutung für Serpentin-Forschung: *Fortschr. Miner.* **39,** 206–324.

McKee, T. R., Dixon, J. B., Whitehouse, U. G., and Harling, D. F. (1973) Study of Te Puke halloysite by a high resolution electron microscope: *31st Ann. Electron Microscopy Soc. of America Meeting.*

Mizota, C. and van Reeuwijk, L. P. (1986) Clay mineralogy and chemistry of Andisols and related soils from diverse climatic regimes: International Soil Reference and Information Centre, Wageningen, The Netherlands, Monograph (in press).

Pauling, L. (1930) The structure of the chlorites: *Proc. Natl. Acad. Sci.* **16,** 578–582.

Roy, D. M. and Roy, R. (1954) Experimental study of the formation and properties of synthetic serpentines and related layer silicate minerals: *Amer. Mineral.* **39,** 957–975.

Van der Gaast, S. J. and Kühnel, R. A. (1986) Effects of different cations and relative humidity on hydration-dehydration mechanisms of Wyoming montmorillonite: *Applied Clay Science* (in press).

Van der Gaast, S. J. and Vaars, A. J. (1981) A method to eliminate the background in X-ray diffraction patterns of oriented clay mineral samples: *Clays & Clay Minerals* **16,** 383–393.

Van der Gaast, S. J., Wada, K., Wada, S.-I., and Kakuto, Y. (1985) Small-angle X-ray diffraction, morphology, and structure of allophane and imogolite: *Clays & Clay Minerals* **33,** 237–243.

Wada, K. and Kakuto, Y. (1983) Intergradient vermiculite-kaolin mineral in a Korean Ultisol: *Clays & Clay Minerals* **31,** 183–190.

Wielemaker, W. G. and Wakatsuki, T. (1984) Properties, weathering and classification of some soils formed in peralkaline volcanic ash in Kenya: *Geoderma* **32,** 21–44.

Zussman, J. (1954) Investigation of the crystal structure of antigorite. *Mineral. Mag.* **30,** 498–512.

(Received 23 November 1985; accepted 4 September 1986; Ms. 1538)